arXiv:hep-ph/0610331v1 25 Oct 2006

Effects of the Running of the QCD Coupling on the Energy Loss in the Quark-Gluon Plasma

Jens Braun[1] and Hans-Jürgen Pirner[1,2]

[1]*Institute for Theoretical Physics, University of Heidelberg, Philosophenweg 19, 69120 Heidelberg, Germany*

[2]*Max-Planck-Institut für Kernphysik, Saupfercheckweg 1, 69117 Heidelberg, Germany*

Finite temperature modifies the running of the QCD coupling $\alpha_s(k,T)$ with resolution k. After calculating the thermal quark and gluon masses selfconsistently, we determine the quark-quark and quark-gluon cross sections in the plasma based on the running coupling. We find that the running coupling enhances these cross sections by factors of two to four depending on the temperature. We also compute the energy loss $\frac{dE}{dx}$ of a high-energy quark in the plasma as a function of temperature. Our study suggests that, beside t-channel processes, inverse Compton scattering is a relevant process for a quantitative understanding of the energy loss of an incident quark in a hot plasma.

I. INTRODUCTION

The consequences of a strongly interacting phase of QCD at high temperatures are currently very actively investigated. The existence of such a phase was suggested in Ref. [1] after a careful analysis of QCD lattice data. Moreover, it has been known for quite a while that perturbative approaches to QCD cannot give final answers to many questions of heavy-ion collision experiments, such as the short thermalization times of the quark-gluon plasma.

High-temperature effective field theory has often used a running QCD coupling depending on the temperature only which may be justified at very high temperatures $T \gg \Lambda_{\rm QCD}$, see e.g. [2]. In current heavy-ion collision experiments, however, the temperature T may not be the only important scale, it is one among others, such as the momenta p of the partons. Therefore the running of the coupling in the momentum regime, where $p \sim T$, has to be taken into account for the computation of cross sections and energy-loss processes. In this

paper we present a first approach in this direction. In Sec. II, we review recently obtained results from a calculation of the strong coupling from first principles within the framework of the functional RG [3, 4, 5]. Moreover, we deduce a parametrization for strong coupling at zero and finite temperature from these results. We use the results from Refs. [3, 4] for a computation of the parton cross section and the energy loss of partons in the quark-gluon plasma in Sec. III and IV, respectively. In particular, we study the energy loss of an incident quark in the quark-gluon plasma incorporating t-channel processes and inverse Compton scattering. Taking the running coupling of QCD into account, we find that the energy loss of an incident quark in a hot plasma is increased. Moreover, our results suggest that inverse Compton scattering gives a third of the energy loss of an incident quark. Our conclusions and future plans are found in Sec. V.

II. RUNNING OF THE STRONG COUPLING

Recently the QCD coupling $\alpha_s(k,T)$ at finite temperature has been calculated by nonperturbative functional Renormalization Group methods [3] and shows a considerable variation with the resolution k. The calculation employs the background-field formalism [6] within the RG framework [5, 7]. The effective action used for the determination of the running coupling includes an infinite power series of the gauge-invariant operator $F^a_{\mu\nu}F^a_{\mu\nu}$:

$$\Gamma_k = \int_x \left\{ \sum_i Z_k^{(i)} \left(F^a_{\mu\nu}F^a_{\mu\nu}\right)^i + \bar{\psi}\not{D}[A]\psi \right\} + \text{gauge-fixing term} + \text{ghost term}. \qquad (1)$$

The truncation of the full effective action includes arbitrarily high gluonic correlators projected onto their small-momentum limit and onto the particular color and Lorentz structure arising from powers of $F^a_{\mu\nu}F^a_{\mu\nu}$. It represents a gradient expansion in the field strength and neglects higher-derivative terms and more complicated color and Lorentz structures. So far possible differences between magnetic and electric terms have not been considered. In the background-field method, the β-function of the running coupling g is related to wave function renormalization of the background field [6] via

$$k\frac{\partial}{\partial k}g^2 = \eta\, g^2 \qquad \text{with} \qquad \eta = -k\frac{\partial}{\partial k}\ln Z_k^{(1)}\,, \qquad (2)$$

as a consequence of the non-renormalization of the product of the background field and the coupling. The coefficient of the first term $Z_k^{(1)}$ in the effective action (1) evolves with the

renormalization scale k, successively driven by all other operators in the action. In Refs. [3, 5] the authors keep track of all contributions from the flows of the $Z_k^{(i)}$ to the flow of the running coupling. They use as initial condition for the coupling the measured value at the τ-mass scale [8], $\alpha_{\rm s} = 0.322$. The resulting β-function at zero temperature agrees well with the perturbative two-loop running in the $\overline{\rm MS}$-scheme at high resolution k. It approaches a strong-coupling fixed point in the infrared (IR) [5] in accordance with results from the Schwinger-Dyson equations and RG flow equations in Landau gauge [9, 10]. At zero temperature, the coupling α_s can be parametrized by

$$\alpha_s(k, T=0) = \frac{\alpha_s^*}{\ln\left(e + \left(\frac{k}{\Lambda_s}\right)^a + \left(\frac{k}{\Lambda_s}\right)^b\right)}\,, \tag{3}$$

where $\alpha_s^* = 5.7$ denotes the value of the IR fixed point and $e = 2.718$. The parameters a, b and Λ_s are given by

$$a = 9.07, \quad b = 5.90 \quad \text{and} \quad \Lambda_s = 0.263\,\text{GeV}\,. \tag{4}$$

Similar parametrizations were also found in studies in terms of Schwinger-Dyson equation [9].

At finite temperature T, the UV behavior remains unaffected for scales $k \gg T$ and agrees well with the perturbative running coupling at zero temperature for high-momentum scales. In the infrared, however, the running is strongly modified compared to results for vanishing temperature: $\alpha_s(k, T)$ reaches a maximum at $k \sim T$ and then decreases towards lower scales, see Fig. 1. This can be easily understood in terms of a simple picture: below the scale $k \sim T$, gluonic fluctuations with a Compton wave length larger than the extent of the Euclidean time direction become effectively three-dimensional. Therefore the limiting behavior of the coupling flow in this regime is governed by the spatial $3d$ Yang-Mills theory. Nontrivial, however, is the fact that the coupling decreases for $k < T$. This is due to the existence of a non-Gaussian IR fixed point in the three-dimensional theory [3, 4]. In the low momentum regime, the solution of the RG-equations gives a linear behavior with a slope determined by the infrared fixed point of the spatial $3d$ Yang-Mills theory [4]:

$$\alpha_s(k \ll T) \approx \alpha_{3d}^* \frac{k}{T} + \mathcal{O}\left(\left(\frac{k}{T}\right)^2\right)\,. \tag{5}$$

It is well known that the low-momentum limit of thermal loops enhances the powers of the coupling as $\alpha_s T/k$. From Eq. (5), we can read off that also the enhanced effective coupling

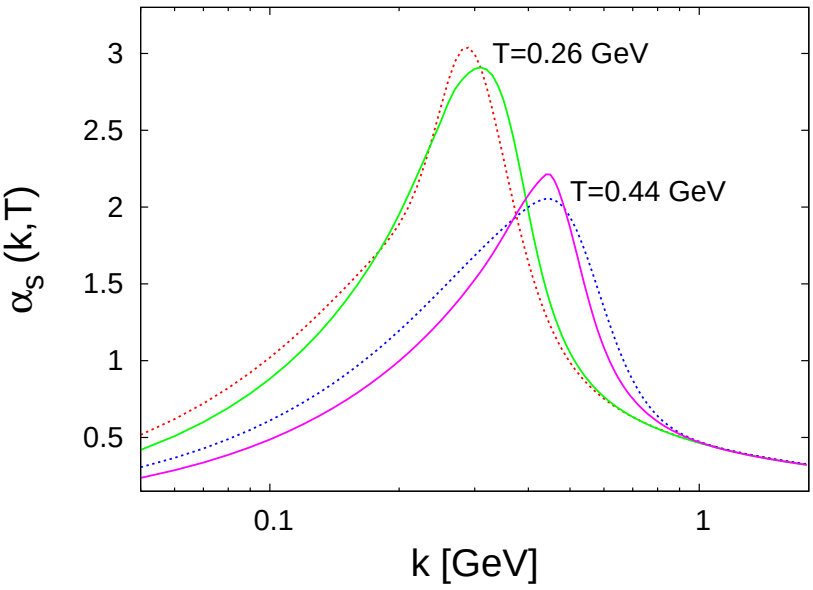

Figure 1: Comparison of the fit of the running coupling (dotted lines) obtained from Eqns. (6) and (9) with the full numerical result (straight line) for pure Yang-Mills theory from Refs. [3, 4] for $T = 0.26$ GeV and $T = 0.44$ GeV.

$\alpha_s T/k$ remains constant for $k \to 0$, similarly to the coupling α_s at zero temperature. We note that the IR fixed point in the $3d$ Yang-Mills theory is also in accordance with recent results in the Landau gauge [11].

A good parametrization of the running coupling at finite temperature which respects the perturbative UV behavior and the $3d$ IR fixed point has the following form:

$$\alpha_s(k,T) = \frac{u_1 \frac{k}{T}}{1+\exp\left(u_2\frac{k}{T}-u_3\right)} + \frac{v_1}{\left(1+\exp\left(v_2\frac{T}{k}-v_3\right)\right)\ln\left(e+\left(\frac{k}{\Lambda_s}\right)^a+\left(\frac{k}{\Lambda_s}\right)^b\right)}\,. \qquad (6)$$

If we choose the parameters a, b and Λ_s to be the same as in Eq. (4), then the above parametrization agrees with this equation at $T = 0$ for

$$v_1 = \alpha_s^* \left(1+\exp\left(-v_3\right)\right). \qquad (7)$$

In order to take the limiting behavior of the coupling for $k \ll T$ into account, we choose

$$u_1 = \alpha_{3d}^* \left(1+\exp\left(-u_3\right)\right). \qquad (8)$$

Here α_{3d}^* and α_s^* denote the values of the IR fixed point of $SU(3)$ Yang-Mills theory in $d = 3$ and $d = 4$ dimensions, respectively. The remaining four parameters fit the numerical results

for pure Yang-Mills theory obtained from the RG equations in Ref. [3]:

$$u_2 = 5.47, \quad u_3 = 6.01, \quad v_2 = 10.13 \quad \text{and} \quad v_3 = 9.27\,. \tag{9}$$

As shown in Fig. 1, the fit is in reasonable agreement with the results of Ref. [3] for temperatures $T \in [0.2\,\text{GeV}, 0.6\,\text{GeV}]$.

Phenomenologically, the strong variation of the running coupling as a function of the resolution k is important. Especially the behavior of the coupling near its maximum value influences physical observables. With increasing temperature the position of the maximum shifts to higher momenta and the value at the maximum decreases. On average, the system becomes less strongly coupled for higher temperature, in agreement with naive expectations from a temperature-dependent effective coupling. This behavior influences the scattering cross section of a quark with the particles in the quark-gluon plasma. As we will discuss below, this elastic cross section contributes significantly to the energy loss of an incident quark in the quark-gluon plasma.

III. EFFECTIVE CROSS SECTION OF AN INCIDENT QUARK

Before we turn to the calculation of the cross sections, we discuss the Debye mass μ_s which enters as screening mass in this calculation. As argued in Ref. [12], the relevant coupling for the calculation of the Debye mass μ_s must be fixed self-consistently at the scale $k = \mu_s$, since in the gluon polarization operator external gluons have vanishing momentum. Therefore we use the following self-consistent equation for the determination of the Debye mass μ_s to leading order [12]:

$$\mu_s^2(T) = \frac{4\pi}{3} N_c \left(1 + \frac{1}{6} N_f\right) \alpha_s(\mu_s(T), T)\, T^2\,. \tag{10}$$

Results for the Debye mass μ_s are shown in Fig. 2 as a function of temperature for three flavors. Here and in the following we identify the scale k^2 set by the RG with the momentum scale p^2. This nontrivial assumption is justified, because the regulator function entering in the calculation of the running coupling specifies the Wilsonian momentum-shell integration in such a way that the RG flow of the coupling is dominated by fluctuations with momenta $p^2 \simeq k^2$.

Since we are interested in temperatures above the critical temperature, the relevant values of the running coupling $\alpha_s^2(\mu_s(T), T)$ in Eq. (10) lie near the asymptotic two-loop scaling

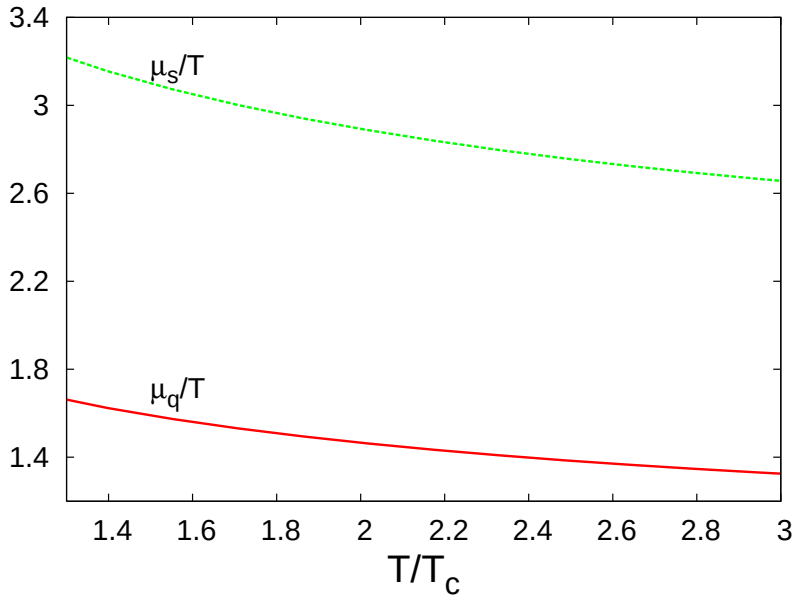

Figure 2: The figure shows the dimensionless ratios of the gluon screening mass μ_s and the quark mass μ_q over temperature T as a function of the dimensionless quantity T/T_c for $N_f = 3$. The chiral phase transition temperature T_c is given in Eq. (13).

region, i.e. above the scale set by temperature T. The mass of the renormalized quark propagator in hot QCD was calculated in Ref. [13]. Along the lines of our calculation of the Debye mass, we use this result for a calculation of an "effective quark mass" μ_q by solving the corresponding self-consistent equation:

$$\mu_q^2(T) = \frac{\pi}{2}\frac{N_c^2-1}{2N_c}\alpha_s(\mu_q(T),T)\,T^2\,. \tag{11}$$

The results for $\mu_s(T)$ as well as $\mu_q(T)$ are shown in Fig. 2 for $N_f = 3$ massless quark flavors. The solutions of the self-consistency equations (10) and (11) exhibit a behavior in form of an alternating series in powers of $\frac{T}{T_c}$:

$$\frac{\mu_j(T)}{T} \approx m_0^{(j)} - m_1^{(j)}\left(\frac{T_c}{T}\right) + m_2^{(j)}\left(\frac{T_c}{T}\right)^2 - m_3^{(j)}\left(\frac{T_c}{T}\right)^3 + \ldots\,, \quad \text{with} \quad j \in \{q,g\}. \tag{12}$$

For our analysis, we use the following chiral phase transition temperatures

$$T_c(N_f=2) \approx 0.186\,\text{GeV} \quad \text{and} \quad T_c(N_f=3) \approx 0.161\,\text{GeV}\,. \tag{13}$$

These values, which were obtained from an RG calculation [4], are in good agreement with lattice QCD studies [14]. The coefficients $m_i^{(j)}$ in Eq. (12) depend on the number of flavors

i	0	1	2	3
$m_i^{(g)}(N_f=2)$	4.31	-1.45	0.40	-0.04
$m_i^{(g)}(N_f=3)$	4.29	-1.15	0.28	-0.02
$m_i^{(q)}(N_f=2)$	2.50	-0.96	0.27	-0.03
$m_i^{(q)}(N_f=3)$	2.32	-0.70	0.17	-0.02

Table I: The fitted values for the coefficients $m_i^{(j)}$ of the power series (12) for $N_f = 2$ and $N_f = 3$.

N_f. The values of these coefficients for a truncated series, including powers up to $(T/T_c)^3$, obtained from a fit to the full numerical data are given in Tab. I.

The Debye mass as well as the "effective quark mass" enter into the calculation of the effective cross section which a fast quark experiences when it traverses the quark-gluon plasma. These masses serve as an infrared cut-off for the cross section. In the following, we neglect the spins of the partons and consider the cross section averaged over initial and summed over final colors of both projectile and target partons. In a first approach, this is a justified assumption for the processes under consideration [15]. Using the temperature-dependent coupling $\alpha_s(p,T)$, the Debye mass $\mu_s(T)$ as well as the "effective quark mass" $\mu_q(T)$, the total cross section of an incident quark obtains

$$\sigma_i(T) = C_i \int_0^s d|t| \, \frac{d\sigma^{t-\text{ch.}}}{d|t|} + \delta_{i(qg)} \int_{\mu_q^2(T)}^s d|u| \, \frac{d\sigma^{\text{IC}}}{d|u|} \qquad (i \in \{qq, qg\}) \, , \tag{14}$$

where the factor C_i denotes the respective color factor which is $C_{qq} = 4/9$ for qq-scattering and $C_{qg} = 1$ for qg-scattering. The differential cross sections for t-channel and u-s-channel processes are given by [15, 16]

$$\frac{d\sigma^{t-\text{ch.}}}{d|t|} = \frac{2\pi\alpha_s^2\left(\sqrt{|t|}, T\right)}{\left(|t| + \mu_s^2(T)\right)^2} \quad \text{and} \quad \frac{d\sigma^{\text{IC}}}{d|u|} = \frac{4\pi}{9s^2}\left(\alpha_s^2\left(\sqrt{s}, T\right)\frac{|u|}{s} + \alpha_s^2\left(\sqrt{|u|}, T\right)\frac{s}{|u|}\right). \tag{15}$$

In the calculation of the quark-gluon cross section we take into account t-channel exchange processes as well as u-s-channel exchange processes, where the latter ones are the only processes possible in QED. They are denoted as inverse Compton-scattering (IC scattering) processes, where a fast fermion hits a thermal boson. In high-energy astrophysics the energy loss of electrons in our galaxy is dominated by scattering on photons of the cosmic-microwave

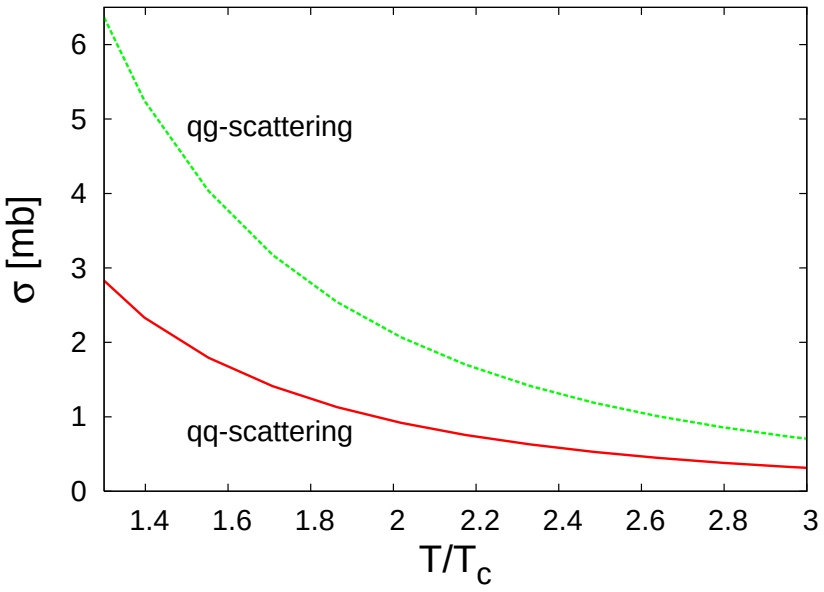

Figure 3: The cross sections for qq and qg-scattering in the quark-gluon plasma are shown as a function of the dimensionless quantity T/T_c for $N_f = 3$ massless quark flavors in the limit $s \to \infty$. The chiral phase-transition temperature is given by $T_c \approx 161$ MeV.

background [17]. Moreover, it is also the main process for the production of high-energy γ-rays [18].

At finite temperatures, the effective differential cross section is enhanced for $p \approx T$ due to the increasing of the running coupling with momentum transfer p. This in turn leads to a larger integrated cross section σ_i itself. The numerical results for the integrated cross sections are given in Tab. II. To be specific, we show the cross section for qq-scattering and qg-scattering in Fig. 3. If one uses the running QCD coupling of Ref. [3] for three massless quark flavors, one gets a qq cross-section of $\sigma_{qq}(T = 1.3\,T_c) \approx 2.79\,\text{mb}$ at $T = 1.3\,T_c$ and of $\sigma_{qq}(T = 3.3\,T_c) \approx 0.24\,\text{mb}$ at $T = 3.3\,T_c$.

For comparison, we have added in Tab. II the calculation of the qq-cross section if the strong coupling would be constant $\alpha_s = 0.5$. The result from our improved calculation is enhanced by a factor of four maximally compared with the calculation using constant α_s. So the mean free path with the running coupling becomes much shorter and even elastic collisions may enter into the energy loss scenario.

$\frac{T}{T_c}$	1.3	1.8	2.3	2.8	3.3
$\sigma_{qg}(T, N_f = 3)$ [mb]	6.29	2.78	1.46	0.86	0.54
$\sigma_{qq}(T, N_f = 3)$ [mb]	2.79	1.23	0.65	0.38	0.24
$\sigma_{qq}(T, N_f = 3, \alpha_s = 0.5)$ [mb]	0.66	0.34	0.21	0.14	0.10

Table II: Total cross section calculated from Eq. (14) in the limit $s \to \infty$ for different values of T/T_c for qq-scattering and qg-scattering of the incident quark. For comparison we also show the results for $\sigma_{qq}(T)$ for $\alpha_s(k, T) = \alpha_s = 0.5$. The chiral phase-transition temperature is given by $T_c \approx 161$ MeV.

IV. JET'S COLLISIONAL ENERGY LOSS

In this section, we discuss the collisional energy loss of an incident quark in a hot plasma which we study with the running coupling depending on temperature and resolution. Ground-breaking work on energy loss of energetic partons in a hot plasma was done by Bjorken [19]. Recently this calculation has been redone with a running coupling in one-loop approximation independent of temperature [20]. We are interested in the energy loss due to elastic scattering of a high-energy quark from a parton of momentum p in the plasma for temperatures $T > \Lambda_{\rm QCD}$. Let us start with the calculation including the cross section for t-channel exchange processes ($t \ll s$).

The cross section for such processes is given in Eq. (15). The energy loss dE of the high-energy quark per length dx in the hot plasma due to t-channel processes can be calculated as [19]

$$\frac{dE_q^{t-\rm ch.}(T)}{dx} = \frac{2}{3} \int d^3p \, \rho_{\rm eff.}(p, T) \, \Phi \int_{t_1}^{t_2} dt \frac{d\sigma^{\rm t\text{-}ch.}}{dt} \nu(p, t) \, . \tag{16}$$

Here Φ denotes the flux factor and $\nu = E - E'$ is the energy difference of the incident and emergent parton depending on the thermal momentum p and the momentum transfer t. Considering the Casimir factors for the various processes, we have defined an effective plasma density $\rho_{\rm eff.}(k, T)$:

$$\rho_{\rm eff.}(p, T) = \frac{2}{3} \, \rho_q(p, T) + \frac{3}{2} \, \rho_g(p, T) \, , \tag{17}$$

where $\rho_q(p,T)$ and $\rho_g(p,T)$ are the quark and gluon momentum distributions, respectively:

$$\rho_q(p,T) = \frac{12N_f}{(2\pi)^3}\frac{1}{\mathrm{e}^{|p|/T}+1} \quad \text{and} \quad \rho_g(p,T) = \frac{16}{(2\pi)^3}\frac{1}{\mathrm{e}^{|p|/T}-1}\,. \tag{18}$$

In our calculation, we take into account that the coupling $\alpha_s(t,T)$ depends on both momentum transfer t and temperature T. Finally, the energy loss will be a function of the temperature and incident energy. Note that the running of α_s was not taken into account by Bjorken and only partially taken into account by a temperature-independent one-loop approximation in Ref. [20]. Following Ref. [19], we can write ν for E, $E' \gg |p|$ as

$$\nu = \frac{|t|}{2p\Phi}\,. \tag{19}$$

Using Eqns. (15), (18) and (19), the energy loss of an incident quark propagating through a hot plasma is determined by

$$\frac{dE_q^{t-\mathrm{ch.}}(T)}{dx} = \frac{4}{3}\,\pi\left(1+\frac{N_f}{6}\right)T^2\int_{|t_2|}^{|t_1|} d|t|\,\frac{\alpha_s^2(\sqrt{|t|},T)}{\left(|t|+\mu_s^2(T)\right)^2}\,|t|\,. \tag{20}$$

In our calculations, we use $|t_1| = s$ and $|t_2| = 0$. Note that the energy of the incident quark E_q and the average value of s are related by $s = 2E_qT$. However, even the limit $|t_1| \to \infty$ would be well-defined since the coupling decreases logarithmically. In Fig. 4 we show the energy loss of a massless quark as a function of T/T_c for different energies E_q of the incident quark due to t-channel exchange processes.

Next, we demonstrate that quark-gluon inverse Compton scattering also gives a quantitatively relevant contribution to the energy loss for a quark traversing the quark-gluon plasma. Along the lines of the t-channel calculation we obtain for the energy loss due to IC-scattering for large s:

$$\frac{dE_q^{\mathrm{IC}}(T)}{dx} \;=\; \frac{8}{27}\pi\,T^2\int_{\mu_q^2(T)}^{s} d|u|\,\left(\alpha_s^2(\sqrt{s},T)\frac{|u|}{s}+\alpha_s^2(\sqrt{|u|},T)\frac{s}{|u|}\right)\frac{s-|u|}{s^2}\,. \tag{21}$$

The results for energy loss due to this process as a function of T/T_c for different energies of the incident quark E_q are shown in Fig. 5 for $N_f = 3$ massless quark flavors. Comparing the results for the t-channel process with the IC process in Fig. 6, we observe that the IC process enhances the energy loss of the incident quark. Intuitively, this is clear since the s-u channel processes are central collisions where the high-energy particle can transfer more energy. However, due to the screening mass of the quark, the largest energy transfers are

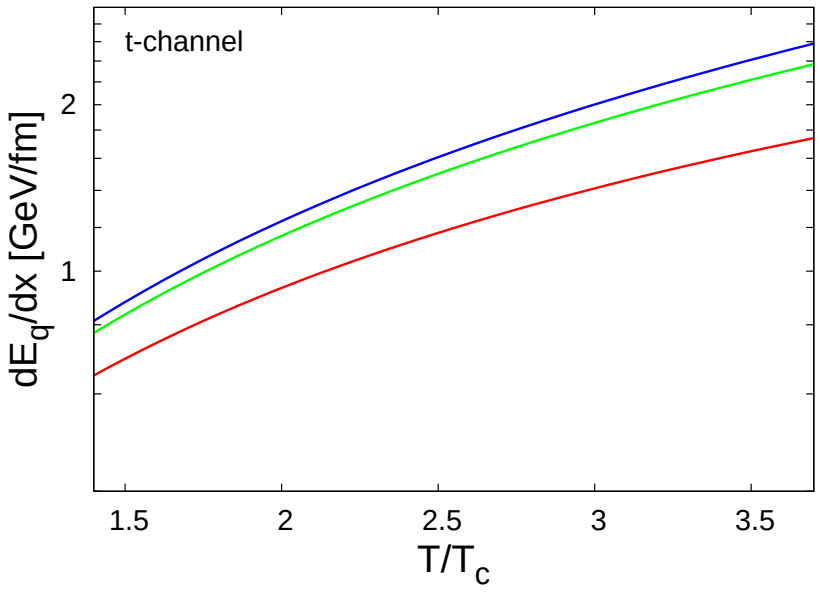

Figure 4: Collisional energy loss of a massless quark in QCD with $N_f = 3$ massless quark flavors due to t-channel gluon exchange as a function of T/T_c. We show the results for energies $E_q = 20,\ 100,\ 200\,\text{GeV}$ of the incident quark (from bottom to top). The chiral phase transition temperature is given by $T_c \approx 161$ MeV.

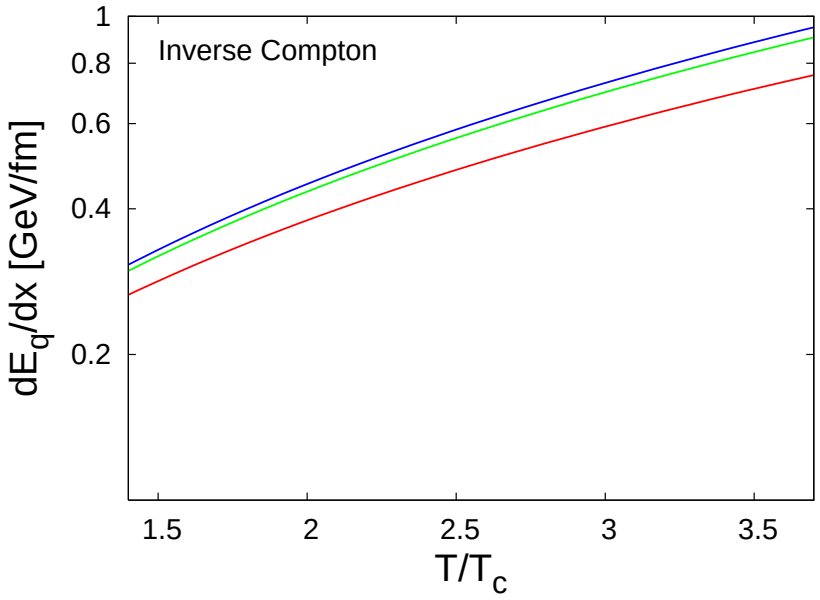

Figure 5: Energy loss of a light quark in QCD with $N_f = 3$ massless quark flavors due to inverse Compton scattering as a function of T/T_c for energies $E_q = 20,\ 100,\ 200$ GeV of the incident quark (from bottom to top). The chiral phase transition temperature is given by $T_c \approx 161$ MeV.

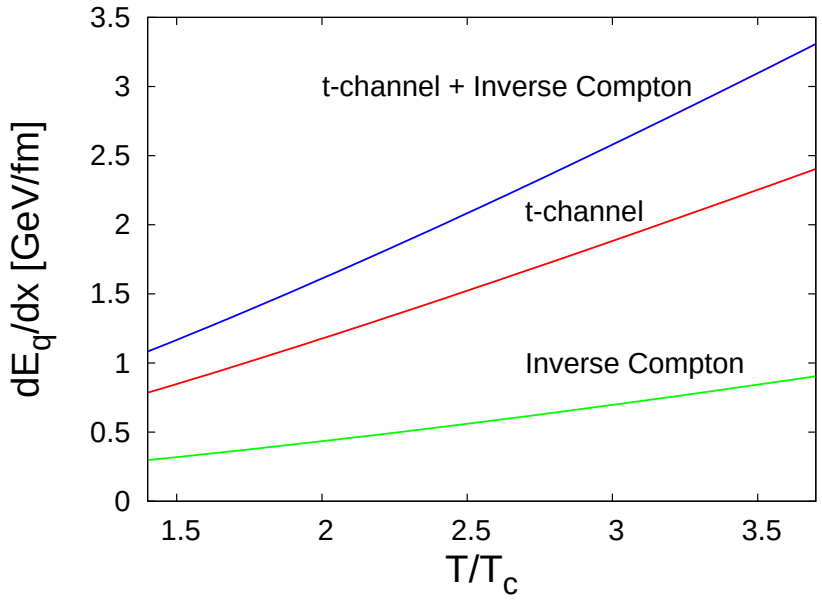

Figure 6: Comparison of energy loss of a massless quark in QCD with $N_f = 3$ massless quark flavors due to inverse Compton scattering and due to t-channel gluon exchange as a function of T/T_c for energies $E_q = 100$ GeV of the incident quark. The chiral phase transition temperature is given by $T_c \approx 161$ MeV.

reduced. As far as we know, this process has not yet been taken into account in previous theoretical work, cf. [21]. Taking a temperature of $T \approx 2\,T_c$, then the IC process gives $\frac{dE}{dx} \approx 0.43$ GeV/fm compared with $\frac{dE}{dx} \approx 1.15$ GeV/fm for the t-channel process. The extra contribution due to the IC process helps to explain the energy loss observed at RHIC which is dominated by the early stages of the collision where the plasma is dense and hot [22]. The collisional energy loss is approximately of the same order as the radiative energy loss [15], since the density of the scatterers is falling very quickly. For a recent discussion of this problem, see also Ref. [21].

V. CONCLUSIONS AND OUTLOOK

We demonstrated that the running of the QCD coupling in the high-temperature plasma is important. The coupling varies as a function of the temperature T and the resolution k. For momenta $|p|$ larger than the temperature T the infrared growth of the coupling enhances the cross sections and the energy loss considerably compared with calculations

with a constant value for the QCD coupling. For momenta $|p| < T$, the coupling decreases due to the existence of a non-Gaussion infrared fixed point of the spatial $3d$ Yang-Mills theory. In fact, this decreasing coupling is only weakly sampled in the calculations because of the screening masses of the quarks and gluons which serve effectively as an IR cutoff. In addition to the effects arising from the running of the QCD coupling, our results suggest that the inverse Compton process is a relevant mechanism for a high-energy quark to lose energy in the quark-gluon plasma. These findings may help to explain the observed energy loss observed at RHIC.

Based on our work presented here, one can estimate a thermalization time. One can approximate the kinetic equation as the scattering of a test particle having a saturation momentum Q_s (≈ 1.5 GeV at RHIC) in a "plasma" of temperature T_0 ($\approx 3\,T_c$) after the time $\tau = \tau_0$, when the colliding nuclei have passed through each other. Explicitly considering that the expansion of the plasma leads to a decrease of T as $T_0(\tau_0/\tau)^{1/3}$, one finds from collisional energy loss an equilibration time of $\tau \approx 4\tau_0$. This time is somewhat shorter than the time found from radiative energy loss [23, 24, 25]. Both mechanisms together seem to give a reasonable short thermalization time, $\tau_{\text{eff.}} \approx 3\,\tau_0$ without involving new mechanisms.

Acknowledgments

The authors are grateful to H. Gies, J. Stachel and K. Zapp for useful discussions. J. B. acknowledges financial support by the Gesellschaft für Schwerionenforschung (GSI) Darmstadt.

---

[1] E. Shuryak, Prog. Part. Nucl. Phys. **53**, 273 (2004)

[2] J. P. M. Blaizot, E. Iancu and A. Rebhan, arXiv:hep-ph/0303185.

[3] J. Braun and H. Gies, arXiv:hep-ph/0512085; (submitted to Phys. Lett. B)

[4] J. Braun and H. Gies, JHEP **0606**, 024 (2006) [arXiv:hep-ph/0602226].

[5] H. Gies, Phys. Rev. D **66**, 025006 (2002); **68**, 085015 (2003).

[6] L. F. Abbott, Nucl. Phys. B **185**, 189 (1981).

[7] M. Reuter and C. Wetterich, Nucl. Phys. B **417**, 181 (1994); M. Reuter and C. Wetterich, Phys. Rev. D **56**, 7893 (1997); F. Freire, D. F. Litim and J. M. Pawlowski, Phys. Lett. B **495**,

256 (2000);

[8] S. Bethke, Nucl. Phys. Proc. Suppl. **135** (2004) 345.

[9] L. von Smekal, R. Alkofer and A. Hauck, Phys. Rev. Lett. **79**, 3591 (1997); D. Atkinson and J. C. Bloch, Mod. Phys. Lett. A **13**, 1055 (1998); C. Lerche and L. von Smekal, Phys. Rev. D **65**, 125006 (2002); C. S. Fischer and R. Alkofer, Phys. Lett. **B536**, 177 (2002).

[10] J. M. Pawlowski, D. F. Litim, S. Nedelko and L. von Smekal, Phys. Rev. Lett. **93**, 152002 (2004); C. S. Fischer and H. Gies, JHEP **0410**, 048 (2004).

[11] A. Maas, J. Wambach, B. Gruter and R. Alkofer, Eur. Phys. J. C **37**, 335 (2004); A. Maas, J. Wambach and R. Alkofer, Eur. Phys. J. C **42**, 93 (2005). [11]

[12] A. Peshier, arXiv:hep-ph/0601119.

[13] R. D. Pisarski, Nucl. Phys. B **309**, 476 (1988).

[14] F. Karsch, E. Laermann and A. Peikert, Nucl. Phys. B **605** (2001) 579.

[15] M. Gyulassy, I. Vitev, X. N. Wang and B. W. Zhang, arXiv:nucl-th/0302077.

[16] R. K. Ellis, W. J. Stirling and B. R. Webber, Camb. Monogr. Part. Phys. Nucl. Phys. Cosmol. **8**, 1 (1996).

[17] V.S. Berezinskii, S.V. Bulanov, V. A. Dogiel, V.L. Ginzburg and V.S. Ptuskin; Astrophysics of Cosmic Rays, p.124 ff.,Amsterdam , 1990

[18] F. A. Aharonian; Very high energy cosmic gamma radiation : a crucial window on the extreme universe, Singapore, 2004.

[19] J. D. Bjorken, FERMILAB-PUB-82-059-THY

[20] A. Peshier, arXiv:hep-ph/0605294.

[21] J. e. Alam, A. K. Dutt-Mazumder and P. Roy, arXiv:nucl-th/0608058.

[22] K. Zapp, G. Ingelman, J. Rathsman and J. Stachel, Phys. Lett. B **637** (2006) 179 [arXiv:hep-ph/0512300].

[23] J. M. Moss *et al.*, arXiv:hep-ex/0109014.

[24] M. B. Johnson *et al.* [FNAL E772 Collaboration], Phys. Rev. Lett. **86**, 4483 (2001) [arXiv:hep-ex/0010051].

[25] M. B. Johnson *et al.*, Phys. Rev. C **65**, 025203 (2002) [arXiv:hep-ph/0105195].